Int. J. Heat Mass Transfer. Vol. 28, No. 1, pp. 147–154, 1985
Printed in Great Britain

0017-9310/85 $3.00 + 0.00

Analysis of boiling heat transfer and two-phase flow in porous media with non-uniform porosity

Y. K. CHUAH and V. P. CAREY
Department of Mechanical Engineering, University of California, Berkeley, CA 94720 U.S.A.

(*Received* 5 *October* 1983 *and in revised form* 8 *May* 1984)

Abstract—An analytical model is presented for the two-phase transport which results from bottom heating of a liquid-saturated porous medium whose porosity varies with height. In this model, the difference between the bottom and the ambient porosity levels is assumed to diminish exponentially. Such a distribution may arise, for example, due to non-uniform distribution of particle sizes in a particle bed. The model applies to flows driven by both buoyancy and capillary effects. Numerical solution of the governing equations for a steam–water system indicates that variation of the porosity profile strongly affects the height of the two-phase zone and the temperature difference across the two-phase layer. Decreasing the porosity locally near the heated surface may increase or decrease the length of the two-phase zone depending on the size of the region of decreased porosity. In addition, decreasing the porosity near the surface is found to significantly increase the temperature difference across the two-phase zone, whereas increasing the porosity at the surface has the opposite effect. The lower-limit of heat flux at which capillary forces affect the two-phase transport has also been calculated. The computed results indicate that even when the region of porosity variation is small, this limit can be changed significantly when the porosity profile near the surface is altered.

INTRODUCTION

BOILING in porous media is an important transport mechanism in a number of technological applications, including thermal energy storage, porous heat pipes, geothermal systems and post-accident analysis of liquid-cooled nuclear reactors. Interest in these applications has prompted a number of studies [1–11] of boiling transport in porous media.

It is now well known that for bottom heating of liquid-saturated porous media, when the temperature of the heating surface slightly exceeds saturation, a two-phase zone of nearly uniform temperature forms above the heating surface. The resulting countercurrent up-flow of vapor and down-flow of condensed liquid is driven by gravity and capillary effects. The convective and phase-change heat transfer in the two-phase zone results in high apparent thermal conductivity.

Several analyses have been proposed for the transport in the two-phase zone. For bottom heating, Bau and Torrance [8] assumed a uniform liquid saturation profile and constant temperature in the two-phase zone. Their analysis, which applies to gravity-driven flows with negligible capillary effects, yielded results in good agreement with experimental measurements. Schubert and Straus [9, 10] have analyzed steam–water counterflow in porous media for conditions characteristic of geothermal systems. They have proposed one-dimensional and two-dimensional models for a steam–water mixture overlying a quiescent pool of water. Their analysis neglected capillary effects but considered the variation of liquid saturation in the two-phase zone.

Ogniewicz and Tien [1] proposed an analytical model that includes both phase-change and capillary effects in the two-phase zone for a one-dimensional heat pipe configuration. Udell [6] developed a similar model with thermodynamic analysis of the two-phase zone and obtained good agreement with experimental measurements [7] for top heating.

All the analytical models described above assume uniform porosity within the porous medium. However, in many applications, the porosity of the matrix may not be uniform. In geothermal systems or porous layers formed after a nuclear accident, the porosity may vary with depth due to variation of the weight of overlying material and/or differential settling of different particle sizes. Athy [12] has modeled the variation of porosity in sedimentary rocks due to compaction with the relation $\varepsilon = \varepsilon_0 e^{-\alpha L}$, where L is the depth below the ground surface.

Porous heat pipe structures may also develop a non-uniform porosity distribution due to plugging of the pores with contaminants or by breakdown and settling of the matrix due to thermal stresses. Although non-uniform porosity distributions may commonly occur, we are aware of no previous attempts to theoretically model boiling in porous media with non-uniform porosity.

The present work is a theoretical analysis of boiling transport in a porous medium with non-uniform porosity. The analysis assumes that the porosity varies only in the vertical (x) direction and that the porosity varies slowly enough so that local conditions are identical to those which would exist if the porosity of the entire medium was equal to the local value. The analysis treats capillary effects in a manner similar to the analyses of Udell [6] and Ogniewicz and Tien [1]. We specifically consider water as the coolant in the medium, although the analysis is quite general and is easily applied to other fluids. Our results indicate that for a given heat flux, the height of the two-phase zone

NOMENCLATURE

A	$= (E/G)^{1/2}$ as in equation (16)
d	mean diameter of the porous material
E	dimensionless profile of porosity
F	dimensionless capillary pressure
G	dimensionless permeability
g	gravitational acceleration
h_{fg}	latent heat of vaporization
k	permeability
k_r	$= d^2$, reference permeability
$\dot{m}$	mass flux
P	pressure
P_c	capillary pressure
$\bar{P}$	dimensionless pressure
P_{l0}	liquid pressure at the heating surface
P_{v0}	vapor pressure at the heating surface
q	heat flux
R	gas constant as in $P = \rho RT$
R_l	relative permeability of liquid
R_v	relative permeability of vapor
T	temperature
v	specific volume
x	vertical coordinate, in upward direction.

Greek symbols

γ	constant in the porosity profile
ε	porosity
ε_r	$= 1$, reference porosity
η	dimensionless vertical coordinate
η_L	length constant in the porosity profile
$\eta_{2\phi}$	dimensionless height of two-phase zone
$\eta_{2\phi 0}$	dimensionless height of two-phase zone for constant porosity ($\gamma = 0$)
θ	$= \dfrac{\theta_l - \theta_{li}}{1-\theta_{li}}$, effective liquid saturation
θ_{li}	irreducible liquid saturation
μ	chemical potential
ν	kinematic viscosity
σ	surface tension
ϕ	$= \dfrac{\nu_l}{\nu_v}$, ratio of kinematic viscosities in liquid and vapor phases
Ω	dimensionless heat flux.

Subscripts

0	condition at the lower boundary
∞	condition at $y = \infty$
l	liquid phase
v	vapor phase
s	saturation condition.

and the temperature difference across the zone may be strongly affected by the porosity variation in the medium.

ANALYSIS

The analysis applies to the two-phase zone that forms when a porous medium saturated with water is heated at the lower boundary. The configuration of the system is shown in Fig. 1. The porosity variation is assumed to be sufficiently weak that Darcy's law, based on the local permeability of the medium, applies to both the liquid and vapor phases. This is expected to be true when the distance over which the porosity varies significantly is large compared with the pore size.

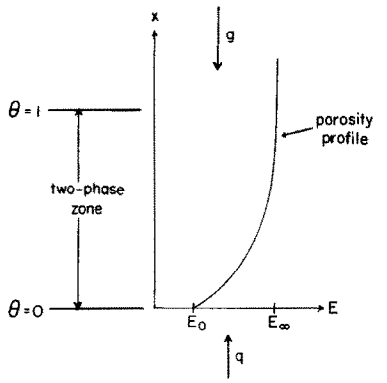

FIG. 1. Configuration of the system.

Mathematically this can be stated as

$$\frac{\varepsilon}{d\varepsilon/dx} \gg d_P \tag{1}$$

where d_P is the mean pore diameter in the medium. When this is valid, Darcy's law in the two-phase region takes the forms

$$\dot{m}_l = -\frac{kR_l}{\nu_l}\left(\frac{dP_l}{dx} + \rho_l g\right) \tag{2a}$$

$$\dot{m}_v = -\frac{kR_v}{\nu_v}\left(\frac{dP_v}{dx} + \rho_v g\right) \tag{2b}$$

where R_l and R_v are the relative permeabilities. Continuity and energy conservation require

$$\dot{m}_l = -\dot{m}_v \tag{3}$$

$$\dot{m}_v h_{fg} = q = -\dot{m}_l h_{fg} \tag{4}$$

where q is the heat flux. Defining the capillary pressure difference

$$P_c = P_v - P_l \tag{5}$$

and using equations (2) to (5) to eliminate $\dot{m}_l$ and $\dot{m}_v$ yields

$$\frac{dP_v}{dx} = \frac{-q\nu_v}{h_{fg}kR_v} - \rho_v g \tag{6a}$$

$$\frac{dP_l}{dx} = \frac{q\nu_l}{h_{fg}kR_l} - \rho_l g \tag{6b}$$

$$\frac{dP_c}{dx} = \frac{-q}{kh_{fg}}\left(\frac{v_v}{R_v} + \frac{v_l}{R_l}\right) + (\rho_l - \rho_v)g. \tag{6c}$$

It is assumed here that the permeability k can be expressed in terms of porosity using the Kozeny–Carman formula

$$k = \frac{d^2}{180}\frac{\varepsilon^3}{(1-\varepsilon)^2} \tag{7}$$

where d is a mean grain size and ε is the porosity. Although this relation strictly applies only to a packed bed of spheres, it is assumed to be qualitatively similar to the dependence of k on ε for other porous structures. The results of the analysis are therefore expected to qualitatively represent the behavior of other porous structures, although the precise numerical values may be different. If the exact relation for $k(\varepsilon)$ is known for a particular matrix, however, it can be inserted into the analysis at this point to obtain more precise results.

The relative permeabilities, R_v and R_l are functions of the local saturation, θ_l. For convenience, a non-dimensional saturation ratio is defined as

$$\theta = \frac{\theta_l - \theta_{li}}{1 - \theta_{li}} \tag{8}$$

where θ_{li} is the irreducible liquid saturation. For R_l and R_v, the following relations are used here which match the experimental data of Wyckoff and Botset [13].

$$R_l = \theta^3 \tag{9}$$

$$R_v = \begin{cases} 1 & \theta \leqslant 0.1 \\ (1.1-\theta)^3, & 0.1 < \theta < 0.9 \\ -0.08(\theta - 0.9) + 0.008 & \theta \geqslant 0.9. \end{cases} \tag{10}$$

The capillary pressure difference, P_c, is also a function of porosity, permeability and surface tension. Leverett [14] has correlated experimental data using the following functional form

$$\frac{P_c}{\sigma}\left(\frac{k}{\varepsilon}\right)^{1/2} = F(\theta) \tag{11}$$

where σ is the surface tension and $F(\theta)$ is the Leverett function. For convenience, we define the following non-dimensional variables

$$\eta = \frac{x(\rho_l - \rho_v)g}{\sigma}\left(\frac{k_r}{\varepsilon_r}\right)^{1/2}, \tag{12}$$

$$\frac{\varepsilon}{k} = \frac{\varepsilon_r E(\eta)}{k_r G(\eta)} \tag{13}$$

$$\phi = \frac{v_l}{v_v} \tag{14}$$

and

$$\Omega = \frac{qv_v}{k_r h_{fg}(\rho_l - \rho_v)g} \tag{15}$$

where ε_r and k_r are reference values of ε and k, respectively. Note that η is the non-dimensional vertical distance from the heating surface. To further simplify the algebra we denote

$$A = \left(\frac{E}{G}\right)^{1/2}. \tag{16}$$

In terms of these variables, equation (6c) becomes

$$\frac{d\eta}{d\theta} = \frac{A(\eta)F'(\theta)}{1 - \dfrac{\Omega}{G(\eta)}\left[\dfrac{1}{R_v(\theta)} + \dfrac{\phi}{R_l(\theta)}\right] - F(\theta)A'(\eta)}. \tag{17}$$

For convenience, we take

$$\varepsilon_r = 1, k_r = d^2 \tag{18}$$

which implies $\varepsilon = E(\eta)$ and $k = d^2 G(\eta)$.

Two kinds of vertical porosity profiles are considered here. In the first type, the porosity is smallest at the heating surface and increases exponentially to a constant value at large η. The second is with maximum porosity at the surface with porosity decreasing exponentially to the ambient value. Therefore, the porosity profile is of the form

$$E = E_\infty[1 - \gamma e^{-\eta/\eta_L}] \tag{19}$$

where

$$\gamma = \frac{E_\infty - E_0}{E_\infty}. \tag{20}$$

The quantities E_∞ and E_0 are the ambient porosity and the porosity at the heating surface, respectively.

For the porosity profiles used, there is a layer of strong porosity variation near the surface. The quantity η_L is a non-dimensional parameter which indicates the characteristic dimension of this layer. Values of η_L considered in this study correspond to conditions in which the porosity varies over 30–100% of the height of the two phase zone.

Using the Kozeny–Carman formula (7), the following equations are obtained for G, A and A'.

$$G(\eta) = \frac{1}{180}\frac{E^3}{(1-E)^2} \tag{21}$$

$$A(\eta) = \sqrt{(180)}\left(\frac{1}{E} - 1\right) \tag{22}$$

and

$$A'(\eta) = -\frac{\sqrt{(180)}E_\infty\gamma}{E^2\eta_L}e^{-\eta/\eta_L}. \tag{23}$$

Finally, $F(\theta)$ must be known in order to solve equation (17). For $F(\theta)$, the correlation proposed by Udell [6] for the imbibition capillary pressure data of Leverett [14] is used, i.e.

$$F(\theta) = 1.417(1-\theta) - 2.120(1-\theta)^2 + 1.263(1-\theta)^3. \tag{24}$$

Introducing the dimensionless liquid and vapor pressures

$$\bar{P}_v = \frac{p_v - p_{v0}}{\sigma}\left(\frac{k_r}{\varepsilon_r}\right)^{1/2} \tag{25}$$

$$\bar{P}_l = \frac{p_l - p_{l0}}{\sigma}\left(\frac{k_r}{\varepsilon_r}\right)^{1/2}. \tag{26}$$

Equations (6a) and (6b) become

$$\frac{d\bar{P}_l}{d\theta} = \frac{d\eta}{d\theta}\left[\frac{\Omega\phi}{GR_l} - 1\right] \tag{27}$$

$$\frac{d\bar{P}_v}{d\theta} = \frac{d\eta}{d\theta}\left[-\frac{\Omega}{GR_v}\right]. \tag{28}$$

The quantities $\bar{P}_{v0}$ and $\bar{P}_{l0}$ in equations (25) and (26) are the pressures of the two phases at $\theta = 0$. They can be determined by imposing the boundary conditions

$$\theta = 1, P_v = P_l = P_\infty, \tag{29}$$

so that

$$P_{v0} = P_\infty - \sigma\bar{P}_v(\theta = 1)/d, \tag{30}$$

$$P_{l0} = P_\infty - \sigma\bar{P}_l(\theta = 1)/d. \tag{31}$$

Equations (17), (27) and (28) are solved with boundary conditions

$$\theta = 0, \quad \eta = 0, \quad \bar{P}_v = \bar{P}_l = 0. \tag{32}$$

The temperature distribution in the two-phase zone is obtained from thermodynamic relations, assuming local thermodynamic equilibrium holds. The local temperature in the two phases are taken to be equal, $T_L = T_v$. As shown by Udell [6], the additional requirement of equal chemical potentials in the two phases yields the following relation between P_l, P_v and T.

$$(P_s(T) - P_l)v_l = R(273.15 + T)\ln\left[\frac{P_s(T)}{P_v}\right] \tag{33}$$

where T is in degrees Celsius. This relation was obtained assuming an incompressible liquid and that the vapor is an ideal gas.

P_l and P_v are calculated from the solutions of equations (27) and (28). Therefore, when P_s as a function of temperature is available, temperature, T, can be determined using equation (33).

In [15], a correlation of P_s and T for water is given as

$$\log_{10} P_s = A - \frac{B}{T + C} \tag{34}$$

where $A = 10.1946, B = 1730.63$ and $C = 233.426$. For better accuracy, equation (34) can be corrected [16] in the following form

$$\log_{10} P_s = A - \frac{B}{T + C} + DT + E\log_{10} T. \tag{35}$$

Then using data from [17], D and E were determined to be

$$D = -1.22066 \times 10^{-4}, \quad E = 6.85300 \times 10^{-3}. \tag{36}$$

In equations (34) and (35), T is in degrees Celsius. The correlation of P_s and T as in equation (35) is accurate to three significant figures in the temperature range from 5°C to 275°C.

NUMERICAL CALCULATIONS

Calculated solutions for the equations described in the previous section were obtained for fixed parameters given below:

$$\left.\begin{aligned} d &= 0.05 \text{ mm} \\ P_\infty &= 1.013 \times 10^5 \text{ N/m}^2 \\ v_l &= 1 \times 10^{-3} \text{ m}^3/\text{kg} \\ R_{H_2O} &= 461.527 \text{ J/kgK} \\ \phi &= 1.460 \times 10^{-2} \\ q &= 1 \text{ kw/m}^2 \\ \Omega &= 3.8107 \times 10^{-4} \end{aligned}\right\}. \tag{37}$$

The ambient porosity, E_∞, was taken to be 0.3 in the numerical solutions with various values of η_L and γ in the ranges 0.5–2.5 and −0.4–0.4, respectively. Recall that negative values of γ correspond to cases with maximum porosity at the surface and positive values of γ correspond to minimum porosity at the surface. When $\gamma = 0$, porosity is constant.

Equations (17), (27) and (28) were solved using a Hammings' modified predictor–corrector method. This is a fourth-order multistep method with integration initiated using a fourth-order Runge–Kutta procedure.

The permeability that results from the values of d and porosity used here is on the order of 1 Darcy (10^{-12} m^2). This value is typical of geological formations of interest in geothermal applications and porous heat pipe structures. This porosity is about an order of magnitude lower than those in the system considered by Bau and Torrance [8]. Consequently, capillary effects, which were negligible in the system of Bau and Torrance [8], will be significant in our system.

RESULTS AND DISCUSSION

The effects of γ and η_L on ΔT and $\eta_{2\phi}$ can be seen in Fig. (2). For positive gradients of porosity, i.e. positive values of γ, the temperature difference across the two-phase zone is found to increase with γ and η_L. Increasing γ and η_L produces a decrease in porosity near the surface in the two-phase zone as seen in equation (19). From the Kozeny–Carman formula (7), it is seen that this results in smaller permeability. To maintain the same mass flow rate of vapor with a smaller permeability requires a higher vapor pressure gradient. Although the height of the two-phase zone, $\eta_{2\phi}$, may increase or decrease with γ depending on η_L, the overall vapor-pressure drop across the zone increases as either γ or η_L are increased. Since temperature is a strong function of P_v, ΔT also increases as γ or η_L are increased.

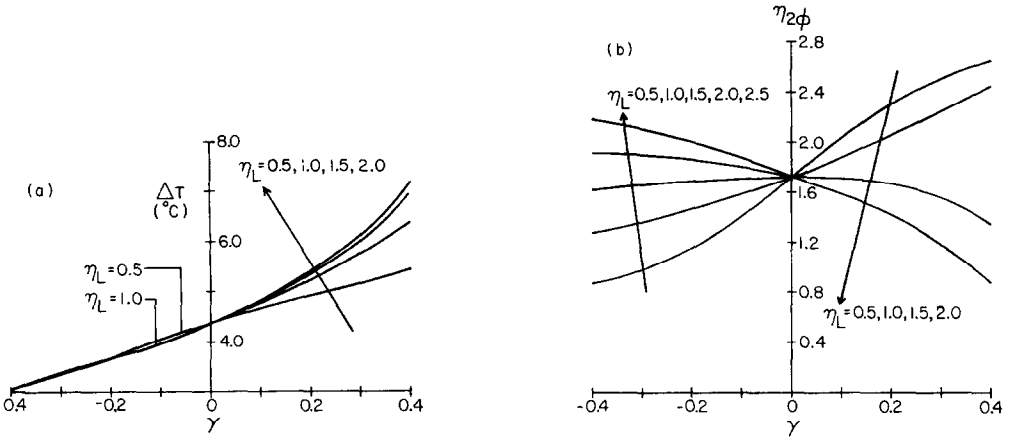

FIG. 2(a) and (b). Height and temperature difference across the two-phase zone for $E_\infty = 0.30$.

For negative values of γ, the porosity is larger near the surface. When $E_\infty = 0.30, E_0 = 0.21$ for $\gamma = 0.3$ and $E_0 = 0.39$ for $\gamma = -0.3$ at the surface. For these conditions, the effect of changing η_L on the temperature difference is small.

The results in Fig. 2(a) also show that for positive γ, the effect of η_L on temperature difference increases with γ. It also indicates that the temperature difference will increase as the porosity gradient near the surface increases. However, the height of the layer of stronger porosity variation near the surface significantly affects the temperature difference only when the porosity gradient is positive. In addition, the effect of η_L on the length of the two-phase zone is seen to increase as γ increases. Calculated results for $E_\infty = 0.25$ with the same γ and η_L values were also obtained which indicated similar trends.

For constant γ, the height of the two-phase zone was found to decrease with η_L for $\gamma > 0$ and increase with η_L for $\gamma < 0$. This result is expected since locally the permeability decreases with η_L for $\gamma > 0$ and increases with η_L for $\gamma < 0$. Lower permeability results in larger resistance to flow and hence a shorter two-phase zone.

On the other hand, for constant η_L, the height of the two-phase zone is found to increase with γ for smaller values of η_L and to decrease with γ at larger values of η_L. There is a transition range, near $\eta_L = 1.5$, where the height of the two-phase zone does not change significantly with γ. Based on these and similar results for $E_\infty = 0.25$, this transition condition was observed to correspond approximately to $\eta_L = 0.8\eta_{2\phi 0}$, where $\eta_{2\phi 0}$, is the height of the two phase zone at $\gamma = 0$.

The phenomenon of the variation of the height of the two-phase zone with γ can be explained in terms of the transport mechanisms in the liquid phase. In the liquid phase, the two important factors in the transport of fluid are capillary effects and permeability. A decrease in porosity will decrease the permeability and hence increase the resistance to the fluid flow. On the other hand, a decrease in porosity will also increase the capillary pressure difference which enhances the transport of liquid. In the transition range, these competing effects offset one another. At small values of η_L, apparently the increase in capillary pressure difference more than compensates for the increased flow resistance, resulting in a longer two-phase zone. For larger values of η_L, the permeability is decreased significantly over a large portion of the two-phase zone. The increased resistance to flow over this larger region more than offsets the increase in capillary pressure

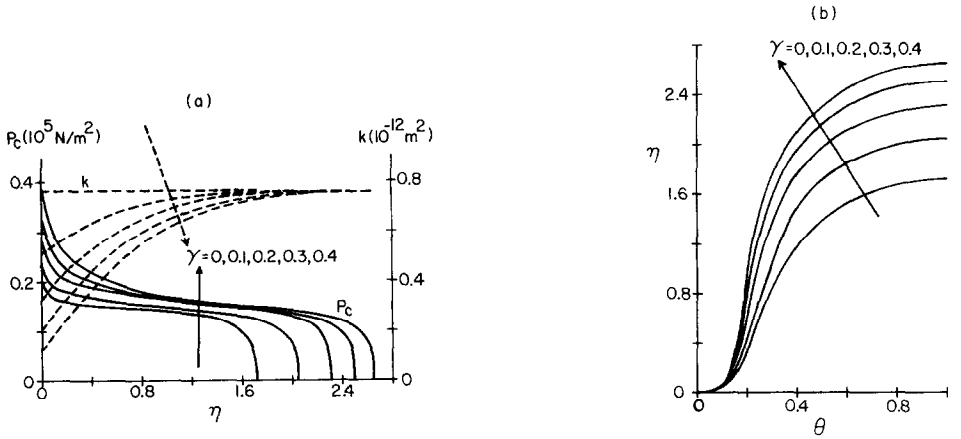

FIG. 3(a) and (b). Variation of θ, P_c and k with η for $E_\infty = 0.30$, $\eta_L = 0.5$ and positive γ.

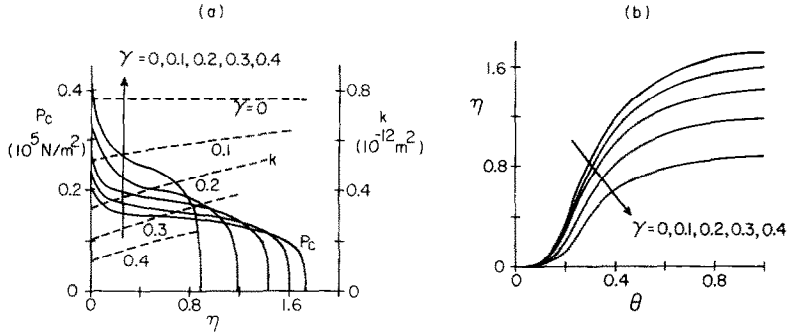

FIG. 4(a) and (b). Variation of θ, P_c and k with η for $E_\infty = 0.30$, $\eta_L = 2.0$ and positive γ.

difference, resulting in a decrease in the height of the two-phase zone.

In Fig. 3, the profiles of P_c, k and θ in the two-phase zone are presented for $E_\infty = 0.30$, $\eta_L = 0.5$ and $\gamma > 0$. The corresponding curves for $\eta_L = 2.0$ are shown in Fig. 4. Note that for $\eta_L = 2.0$, increasing γ decreases the permeability over a greater portion of the medium than for $\eta_L = 0.5$. As discussed previously, this produces added resistance to flow over a larger portion of the matrix at $\eta_L = 2.0$.

The profiles of P_c and k for $E_\infty = 0.30$ and $\gamma < 0$ are shown in Fig. 5 for $\eta_L = 0.5$ and in Fig. 6 for $\eta_L = 2.5$. For $\eta_L = 2.5$, as γ becomes more negative, the porosity increases over a large portion of the medium. This causes an increase in the height of the two-phase region despite a reduction of the capillary pressure at $\eta = 0$. At $\eta_L = 0.5$, the porosity increases near the surface as the value of γ becomes more negative. This decreases the capillary pressure at $\eta = 0$ with little reduction in the resistance to flow over most of the medium. The net result is a reduction in the height of the two-phase zone.

If equation (17) is solved for progressively smaller values of Ω, eventually a value of Ω is reached at which

$$\Omega = \Omega_{\min} = \frac{G(\eta)}{\dfrac{1}{R_v(\theta)} + \dfrac{\phi}{R_l(\theta)}}[1 - F(\theta)A'(\eta)] \quad (38)$$

at some value of η. Note in equation (17) that at this condition $|d\eta/d\theta| \to \infty$. For the constant porosity case, Udell [7] has shown that this singularity represents the minimum Ω (and minimum heat flux) at which capillary forces significantly affect the transport. For Ω values below this limit, $d\theta/d\eta$ may become zero at some location above the heated surface. Beyond this vertical location, a two-phase zone of unlimited height may exist in which liquid and vapor motion are driven by buoyancy alone. The boiling circumstances studied by Bau and Torrance [8] were buoyancy-dominated flows of this type.

When ε is constant, $G(\eta)$ is constant, $A'(\eta)$ is zero and (38) reduces to a form that is equivalent to that obtained by Udell [7] for the constant porosity circumstance. Since the right-side of (38) depends only on θ when the porosity is constant, $\Omega_{\min}$ can be determined by

$$\left(\frac{\Omega_{\min}}{G}\right)_{\varepsilon = \text{const.}} = \max\left\{\frac{R_v(\theta)R_l(\theta)}{R_l(\theta) + \phi R_v(\theta)}\right\}. \quad (39)$$

It is interesting to note that (39) is identical to the relation obtained by Bau and Torrance [8] for the maximum heat flux that can be transferred in the buoyancy-dominated regime without dryout occurring at the surface. This suggests that when $\Omega_{\min}$ is exceeded, buoyancy alone can no longer drive the transport. The length of the two-phase zone then diminishes from an unlimited value for $\Omega < \Omega_{\min}$, to a value dictated by capillary effects, which now also help drive the flow. Depending on the boundary conditions on the porous medium, the transition to a finite two-phase zone length may also result in dry-out at the surface.

To determine $\Omega_{\min}$ for a variable porosity system with

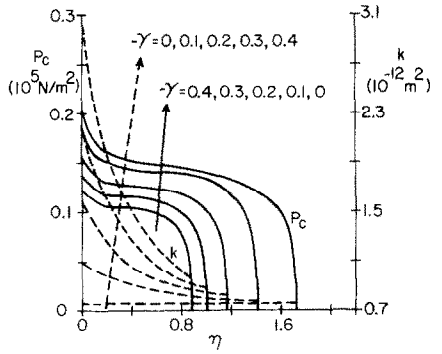

FIG. 5. Variation of P_c and k with η for $E_\infty = 0.30$, $\eta_L = 0.5$ and negative γ.

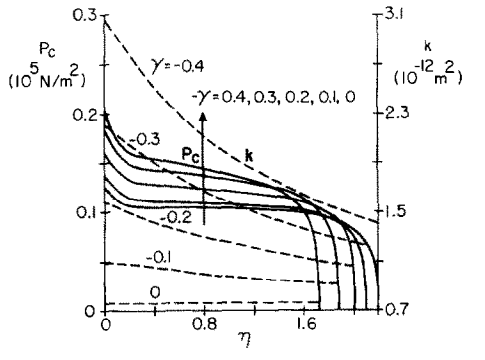

FIG. 6. Variation of P_c and k with η for $E_\infty = 0.30$, $\eta_L = 2.5$ and negative γ.

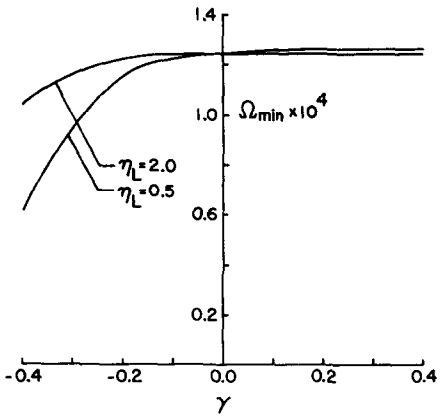

FIG. 7. Computed values of Ω_{min} for various γ and η_L.

given values of γ, η_L and E_∞, equation (17) was solved for progressively smaller values of Ω. For each solution, Ω_{min} was calculated at each step of the integration using (38). As Ω is decreased, Ω_{min} is the value of Ω at which Ω_{min} given by (38) first equals Ω at some point in the layer. For decreasing Ω, this is the first value at which a singularity in $d\eta/d\theta$ is found. Values of Ω_{min} were numerically determined in this manner for various combinations of γ and η_L with $E_\infty = 0.30$. The resulting Ω_{min} values are shown in Fig. 7.

In Fig. 7, it can be seen that $\gamma > 0$ produces virtually no change in Ω_{min}, whereas $\gamma < 0$ produces a slight decrease in Ω_{min}. In equation (38), a positive value of γ increases $|A'|$, and since $F > 0$ and $A' < 0$, this increases Ω_{min}. However, a positive γ decreases G over much of the layer, which tends to decrease Ω_{min}. These effects tend to offset each other, and for $\gamma > 0$, they apparently cancel almost completely. For negative γ, the arguments cited above reverse, with the effects still tending to cancel. However, for $\gamma < 0$, it appears that the net effect is a reduction in Ω_{min}. In physical terms, the limit of Ω below which capillary effects are not important, Ω_{min}, depends on both the porosity and the gradient of porosity, through $A'(\eta)$. For the porosity profiles chosen here, the effects of these dependencies tend to cancel. The change in Ω_{min} is determined by the difference between them.

CONCLUSIONS

The results of the present analysis strictly apply only for a porosity profile of the form $\varepsilon = E_\infty[1-\gamma e^{-\eta/\eta_L}]$ and for media which obey the Kozeny–Carman relation equation (7). However, the qualitative behavior indicated by the results is expected to apply to a broader range of porous media. For other specific systems, the present analysis can easily be extended by including different porosity profiles and functional relations between permeability and porosity.

For the water-saturated system considered here, our results indicate that the temperature difference across the two-phase zone increases with increasing η_L for $\gamma > 0$. However, for $\gamma < 0$, the effect of η_L on ΔT was small. For constant values of η_L, the effect of γ on the height of the two-phase zone varies considerably, depending on the value of η_L. For large η_L values, increasing γ produces a decrease in the height of the two-phase zone. At lower η_L values, increasing γ caused an increase in the height of the two-phase zone.

Apparently, at large η_L, the increase in flow resistance which accompanies a reduction in porosity (increasing γ) more than compensates for the associated increase in capillary pressure. This produces a net decrease in the height of the two-phase zone. At small η_L, the increase in capillary pressure is obtained with only a small increase in the resistance to flow, producing a net increase in the height of the two phase zone. For $\eta_L \simeq 0.8\ \eta_{2\phi 0}$, the effect of the increase in capillary pressure just about balances the increased resistance to flow and changing γ produces little or no change in the height of the two-phase zone.

The value of Ω below which capillary effects are negligible, Ω_{min}, was also calculated for the variable porosity circumstances considered here. The calculated results indicate that for $\gamma > 0$, there is virtually no change in Ω_{min} relative to its value at $\gamma = 0$ (constant porosity). For $\gamma < 0$, decreasing γ is found to reduce Ω_{min}. The weak variation of Ω_{min} with γ for $\gamma > 0$ is attributed to the simultaneous dependence of Ω_{min} on the porosity and porosity gradient. For the porosity profile assumed here, the effect of the porosity gradient on Ω_{min} tends to offset the effect of the associated local change in porosity. The resulting net change in Ω_{min} is small for $\gamma > 0$.

Acknowledgements—The authors wish to acknowledge support for this research by the National Science Foundation under research grant MEA-8307212. The efforts of Mrs J. Reed and Ms L. Donahue in preparation of the manuscript are also appreciated.

REFERENCES

1. Y. Ogniewicz and C. L. Tien, Porous heat pipe, *AIAA Progr. Astronaut. Aeronaut.* **70**, 329–345 (1980).
2. Y. Ogniewicz and C. L. Tien, Analysis of condensation in porous insulation, *Int. J. Heat and Mass Transfer* **24**, 421–429 (1981).
3. E. E. Gomaa and W. H. Somerton, The behavior of multifluid-saturated formations, Part II: Effect of vapor saturation—heat pipe concept and apparent thermal conductivity, SPE paper 4896-B, presented at the Society of Pet. Engineers California Regional Meeting, San Francisco California (April 1974).
4. C. H. Sondergeld and D. L. Turcotte, Flow visualization studies of two-phase thermal convection in a porous layer, *Pure appl. Geophys.* **117**, 321–330 (1978).
5. K. S. Udell, The thermodynamics of evaporation and condensation in a porous media, California Regional Meeting of the Society of Petroleum Engineers San Francisco, California (March 1982).
6. K. S. Udell, Heat transfer in porous media heated from above with evaporation, condensation and capillary effects, ASME *J. Heat Transfer* **105**, 485–492 (1983).
7. K. S. Udell, Heat transfer in porous media considering phase change and capillarity—the heat pipe effect, *Int. J. Heat Mass Transfer* (in press).
8. H. Bau and K. E. Torrance, Boiling in low-permeability

porous materials, *Int. J. Heat Mass Transfer* **25**, 45–55 (1982).
9. G. Schubert and J. M. Straus, Steam–water counterflow in porous media, *J. Geophys. Res.* **84**, 1621–1628 (1979).
10. G. Schubert and J. M. Straus, Two-phase convection in a porous medium, *J. Geophys. Res.* **82**, 3411–3421 (1977).
11. L. M. Cathles, An analysis of the cooling of intrusives by ground-water convection which includes boiling, *Econ. Geol.* **72**, 804–826 (1977).
12. L. F. Athy, Density, porosity and compaction of sedimentary rocks, *Bull. Amer. Ass. Petrol. Geol.* No. 1 **14**, 1–24 (1930).
13. R. D. Wyckoff and H. G. Botset, Fluid flow through unconsolidated sand, *Physics* **7**, 332 (1936).
14. M. C. Leverett, Capillary behavior in porous solids, *AIME Trans.* **142**, 152 (1941).
15. J. Gmehling, and U. Onken, Vapor–liquid equilibrium data collection, Vol. 1, Dechema, Frankfurt, Germany (1977).
16. J. M. Smith and H. C. Van Ness, *Introduction to Chemical Engineer Thermodynamics*, 3rd edn, McGraw–Hill (1975).
17. T. F. Irvine, Jr. and J. P. Hartnett, *Steam and Air Tables in SI units*, McGraw–Hill (1978).
18. J. Bear, *Dynamics of Fluids in Porous Media*, American Elsevier, New York (1972).
19. M. R. J. Wyllie, Relative Permeability, Chapter 25, *Petroleum Production Handbook*, Vol. 2 (edited by Frick) McGraw–Hill, New York (1962).

ANALYSE DU TRANSFERT THERMIQUE PAR EBULLITION ET DE L'ECOULEMENT DIPHASIQUE DANS DES MILIEUX POREUX DE POROSITE NON UNIFORME

Résumé—On présente un modèle analytique du transfert diphasique qui résulte du chauffage à la base d'un milieu poreux saturé de liquide et dont la porosité varie avec la hauteur. Dans ce modèle, la différence de niveau de porosité entre la base et le sommet diminue exponentiellement. Une telle distribution peut être due, par exemple, à une distribution non uniforme de la taille des particules dans un lit. Le modèle s'applique aux écoulements provenant des forces d'Archimède et des capillarités. La solution numérique des équations pour un système eau–vapeur d'eau montre que la variation de porosité affecte fortement la hauteur de la zone diphasique et la différence de température à travers elle. Une décroissance de porosité localement proche de la surface chauffée peut augmenter où diminuer la longueur de la zone diphasique suivant la dimension de la région de porosité faible. De plus, la décroissance de la porosité près de la surface augmente sensiblement la différence de température à travers la zone diphasique, tandis que l'accroissement de la porosité à la surface a un effet contraire. La limite inférieure de flux thermique à laquelle les forces capillaires affectent le transfert diphasique a été calculée. Les résultats du calcul montrent que même lorsque la région de variation de porosité est petite, cette limite peut être fortement modifiée quand le profil de porosité près de la surface est altéré.

UNTERSUCHUNG VON WÄRMEÜBERGANG UND ZWEIPHASENSTRÖMUNG BEIM SIEDEN IN PORÖSEN MEDIEN VON UNGLEICHFÖRMIGER POROSITÄT

Zusammenfassung—Für Zweiphasentransportvorgänge wird ein analytisches Modell erstellt. Diese Vorgänge treten auf, wenn ein flüssig-gesättigtes, poröses Medium mit höhenabhängiger Porosität von unten beheizt wird. In dem Modell nimmt der Unterschied der Porosität zwischen der Unterseite und der Umgebung exponentiell ab. Eine derartige Verteilung kann beispielsweise von einer ungleichmäßigen Verteilung der Partikelgrößen in einem Partikelbett herrühren. Das Modell läßt sich auf Strömungen anwenden, die durch Auftriebs- oder Kapillar-Effekte angetrieben werden. Die numerische Lösung der bestimmenden Gleichungen für ein Dampf-Wasser-System zeigt an, daß Änderungen des Porositätsprofiles die Höhe der Zweiphasenzone und die Temperaturdifferenz in der Zweiphasenschicht stark beeinflussen. Wenn die örtliche Porosität nahe der Heizfläche kleiner wird, kann die Länge der Zweiphasenzone je nach Ausdehnung des Gebietes mit verringerter Porosität zu- oder abnehmen. Zusätzlich zeigt sich, daß eine Verringerung der Porosität nahe der Heizfläche die Temperaturdifferenz in der Zweiphasenzone merklich vergrößert. Darüber hinaus wurde die Untergrenze derjenigen Wärmestromdichte berechnet, bei der Kapillarkräfte den Zweiphasentransport gerade noch beeinflussen. Die Ergebnisse zeigen, daß sich diese Grenze selbst dann, wenn das Gebiet mit veränderter Porosität klein ist, merklich ändern kann, sobald das Porositätsprofil nahe der Heizfläche verändert wird.

АНАЛИЗ ТЕПЛОПЕРЕНОСА ПРИ КИПЕНИИ И ДВУХФАЗНОМ ТЕЧЕНИИ В ПОРИСТЫХ СРЕДАХ С НЕОДНОРОДНОЙ ПОРИСТОСТЬЮ

Аннотация—Представлена аналитическая модель двухфазного переноса, возникающего при нагревании снизу насыщенной жидкостью пористой среды с переменной по высоте пористостью. Модель предполагает экспоненциальное убывание пористости. Такое распределение может иметь место, например, при неравномерном распределении частиц слоя по размерам. Эта модель применима к течениям, вызванным как плавучестью, так и капиллярными эффектами. Численное решение основных уравнений для паро-водяных систем показывает, что изменение профиля пористости сильно влияет на высоту двухфазной зоны и разность температур поперек двухфазного слоя. Локальное снижение пористости у нагреваемой поверхности может увеличить или уменьшить длину двухфазной зоны в зависимости от размера области пониженной пористости. Кроме того, найдено, что уменьшение пористости среды вблизи поверхности существенно увеличивает разность температур поперек двухфазной зоны, в то время как увеличение пористости оказывает противоположный эффект. Рассчитан также нижний предел теплового потока, при котором капиллярные силы оказывают влияние на двухфазный перенос. Результаты расчетов показывают, что даже в том случае, когда область изменения пористости имеет небольшие размеры, этот предел может значительно измениться, если изменится профиль пористости у поверхности.